

Surfing on the edge: chaos versus near-integrability in the system of Jovian planets

Wayne B. Hayes[★]

Computer Science Department, University of California, Irvine, CA 92697-3435, USA

Accepted 2008 January 25. Received 2008 January 17; in original form 2007 October 18

ABSTRACT

We demonstrate that the system of Sun and Jovian planets, integrated for 200 Myr as an isolated five-body system using many sets of initial conditions all within the uncertainty bounds of their currently known positions, can display both chaos and near-integrability. The conclusion is consistent across four different integrators, including several comparisons against integrations utilizing quadruple precision. We demonstrate that the Wisdom–Holman symplectic map using simple symplectic correctors as implemented in MERCURY 6.2 gives a reliable characterization of the existence of chaos for a particular initial condition only with time-steps less than about 10 d, corresponding to about 400 steps per orbit. We also integrate the canonical DE405 initial condition out to 5 Gyr, and show that it has a Lyapunov time of 200–400 Myr, opening the remote possibility of accurate prediction of the Jovian planetary positions for 5 Gyr.

Key words: celestial mechanics – ephemerides – Solar system: general.

1 INTRODUCTION

Both the man of science and the man of art live always at the edge of mystery, surrounded by it. Both, as a measure of their creation, have always had to do with the harmonization of what is new with what is familiar, with the balance between novelty and synthesis, with the struggle to make partial order in total chaos.

J. Robert Oppenheimer

When one speaks of the stability of our Solar system, one must carefully define the meaning of ‘stable’. We say that the Solar system is practically stable if, barring interlopers, the known planets remain gravitationally bound to the Sun and suffer no close encounters between themselves or the Sun, over the main-sequence lifetime of the Sun. In a practically stable Solar system, the orbital eccentricities, inclinations and semimajor axes of all the planets remain within some bounded region, not too far from their present values. In this sense, work by many authors over the past 15 yr has all but proven that the Solar system is practically stable (Laskar 1994, 1996, 1997; Ito & Tanikawa 2002). Good reviews exist (Lissauer 1999; Lecar et al. 2001), and we will not discuss it further in this paper. A second, more formal definition involves the question of whether the Solar system is chaotic or not. In a chaotic system, nearby solutions tend to diverge from each other exponentially with time, although in a weakly chaotic system such as the Solar system, the exponential divergence can be preceded by an initial period of polynomial divergence. Let $d(t)$ be the distance between two solutions, with $d(0)$ being their initial separation. Then $d(t)$ increases approximately as

$d(0)e^{\lambda t}$ in a chaotic system, where λ is the Lyapunov exponent. The inverse of the Lyapunov exponent, $1/\lambda$, is called the Lyapunov time, and measures how long it takes two nearby solutions to diverge by a factor of e . A system that is not chaotic is called integrable or regular, and has a Lyapunov exponent of zero. A practical consequence of being chaotic is that small changes become exponentially magnified, so that uncertainties in the current positions of the planets are magnified exponentially with time. Even though the Solar system is practically stable, a positive Lyapunov exponent means that uncertainties in the current positions of the planets are magnified to the point that we cannot predict the precise positions of the planets in their orbits after a few (or at most a few tens of) Lyapunov times.

KAM (Kolmogorov–Arnold–Moser) theory tells us that essentially all Hamiltonian systems which are not integrable are chaotic. An initial condition (IC) not lying precisely on a KAM torus will eventually admit chaos, but with a time-scale that depends critically on the IC. Symplectic integrators (Channell & Scovel 1990; Wisdom & Holman 1991; Sanz-Serna 1992) have many nice properties when used for long-term integrations of Hamiltonian systems, such as conservation of phase-space volume, and bounded energy error. However, the validity of symplectically integrated numerical solutions also depends critically upon the integration time-step h , with the longevity of the solution’s validity scaling as $e^{a/h}$ for some constant a (Benettin & Giorgilli 1994; Reich 1999). For linear problems, the dependence is even stronger and manifests itself as a bifurcation in the Lyapunov exponent, going discontinuously from zero to a non-zero value (Lessnick 1996; Newman & Lee 2005 – but see Rauch & Holman 1999). Since the Solar system is not integrable, and experiences unpredictable small perturbations, it cannot lie permanently on a KAM torus, and is thus chaotic. The

[★]E-mail: wayne@ics.uci.edu

operative question is the time-scale of the chaos. To compute the time-scale accurately, we must be confident that the measured time-scale is not an artefact of the integration method.

What is the Lyapunov time of the Solar system? Sussman & Wisdom (1988) first demonstrated that the motion of Pluto is chaotic with a Lyapunov time of about 20 Myr, corroborated over a longer integration later by Kinoshita & Nakai (1996). Laskar (1989) performed an averaged integration of the eight major planets (excluding Pluto) and found that the Lyapunov time was about 5 Myr, with the divergence dominated by that of the inner planets. Laskar (1990) believed that secular resonances are the cause of the chaos in the inner Solar system (but see Murray & Holman 2001), although he did not believe the system of Jovian planets was affected by the chaos displayed by the inner planets. Sussman & Wisdom (1992) performed a full (non-averaged) integration of the entire Solar system and confirmed Laskar’s 5 Myr Lyapunov time, and further found that the system of Jovian planets by itself had a Lyapunov time of between 7 and 20 Myr, although their measurement of the Lyapunov time displayed a disturbing dependence on the time-step of the integration. This dependence was later discovered to be due to symplectic integration schemes effectively integrating a slightly different set of ICs; the effect can be corrected (Saha & Tremaine 1992; Wisdom, Holman & Touma 1996), although it decreases with decreasing time-step.

Since there are no two-body resonances amongst the Jovian planets, the cause of the chaos between them was not understood until Murray & Holman (1999) identified the cause as being the overlap of three-body resonances. Murray & Holman (1999) also performed Lyapunov time measurements on a large set of outer Solar systems differing only in the initial semimajor axis of Uranus. They found that their three-body resonance theory correctly predicted which regions of ICs were chaotic, and which were not, at least over the 200-Myr integration time-span they used. For the ‘actual’ Solar system, they found that the Lyapunov time was about 10 Myr. Guzzo (2005) went on to corroborate the three-body resonance theory by performing a large suite of integrations, numerically detecting a large web of three-body resonances in the outer Solar system.

Murray & Holman (1999) noted that the widths $\Delta a/a$ of the individual resonant zones was of order 3×10^{-6} , so that changes in the ICs of that order can lead to regular motion. They note, however, that “the uncertainties in the ICs, and those introduced by our numerical model, are comfortably smaller than the width of the individual resonances, so [the outer] Solar system is almost certainly chaotic.” Given that Guzzo (2005) has also detected many three-body resonances consistent with Murray & Holman’s theory, it would seem at first glance that chaos in the outer Solar system is a fact.

However, the conclusion that the isolated outer Solar system is chaotic cannot be taken for granted. For example, it is known that symplectic integration with too large a time-step can inject chaos into an integrable system (Herbst & Ablowitz 1989; Newman et al. 2000). Although most authors verify their primary results by performing ‘checking’ integrations with smaller time-steps, the checking integrations are not always performed for the full duration of the main integrations. This, combined with the fact that longer symplectic integrations require shorter time-steps (Benettin & Giorgilli 1994; Reich 1999) means that one cannot assume that a time-step good enough, for example, for a 100-Myr integration is also good enough for a 200-Myr integration. There is currently no known method for analytically choosing a short-enough time-step a priori, and so the only method of verifying the reliability of an integration is to reperform the entire integration with shorter-and-shorter time-steps until the results converge. Newman et al. (2000) used this

method to demonstrate that, for a given set of ICs, the Wisdom & Holman (1991) symplectic mapping with a 400-d time-step (about 11 steps per orbit, a commonly quoted time-step) admits chaos, but that the results converge to regularity for any time-step less than about 100 d. However, many authors who find chaos have also performed reasonable convergence tests, demonstrating that the chaos does not always disappear at convergence.

There exists compelling evidence for the absence of chaos in the outer Solar system. Laskar and others noted that when the entire Solar system is integrated, the inner Solar system manifests chaos on a 5-Myr time-scale, but the outer Solar system appears regular in these integrations. Although Laskar’s approximate theory can overlook some causes of chaos, there also exist full-scale integrations that indicate the absence of chaos. Grazier et al. (1999) and Newman et al. (2000) utilized an Störmer integrator with optimal local error properties (see the description of NBI in Section 2) and performed 16 integrations of the Jovian planets lasting over 800 Myr, and found no chaos. Varadi, Runnegar & Ghil (2003) performed a 207-Myr integration of the entire Solar system, down to the effects of the Moon both explicitly as a separate body, and implicitly using some analytic approximations that well approximated the effects of the explicitly integrated Moon. They placed a lower bound of 30 Myr on the Lyapunov time of the system of Jovian planets.

We are thus left with the disturbing fact that, utilizing ‘best practices’ of numerical integration, some investigators integrate the system of Jovian planets and find chaos, while others do not.

In this paper, we demonstrate that this apparent dilemma has a simple solution. Namely, that the boundary, in phase space, between chaos and near-integrability is finer than previously recognized. In particular, the current observational uncertainty in the positions of the outer planets is a few parts in 10^7 (Morrison & Evans 1998; Standish 1998). Within that observational uncertainty, we find that some ICs lead to chaos while others do not. So, for example, drawing seven-digit ICs from the same ephemeris at different times, one finds some solutions that are chaotic, and some that are not. Thus, different researchers who draw their ICs from the same ephemeris at different times can find vastly different Lyapunov time-scales.

2 METHODS

With the exception of the two sets of ICs we have received from other authors (Murray & Holman 1999; Grazier et al. 2005) and the set included in MERCURY 6.2 (Chambers 1999), all ICs used in this paper are drawn at various epochs from DE405 (Standish 1998), which is the latest planetary ephemeris publicly available from Jet Propulsion Laboratory (JPL). It has stated uncertainty for the positions and masses of the outer planets of a few parts in 10^7 . To ensure that our integration agrees over the short term with DE405, we verified in several cases that we can integrate between different sets of DE405 ICs, separated by as much as 100 yr, while maintaining at least seven digits of agreement with DE405.

We integrate the system of Jovian planets using only Newtonian gravity. The inner planets are accounted for by adding their masses to the Sun and perturbing the Sun’s position and linear momentum to equal that of the Sun–Mercury–Venus–Earth–Mars system. This ensures that the resonances between the outer planets is shifted by an amount that is second order in this mass ratio, roughly 3×10^{-11} (Murray & Holman 1999), which is far smaller than the uncertainty in the outer-planet positions. We assume constant masses for all objects and ignore many effects which are probably relevant over a 200-Myr time-scale (see for example Laskar 1999). We account for solar mass loss at a rate of $\dot{m}/m \approx 10^{-7} \text{ Myr}^{-1}$ (Laskar 1999;

Noerdlinger 2005), but note that we observe no noticeable difference if we keep the solar mass constant.

To reduce the possibility that our results are dependent on the integration scheme, we used three different numerical integration methods to verify many of our results in this paper. First, we used the MERCURY 6.2 package (Chambers 1999), with the Wisdom–Holman (Wisdom & Holman 1991) symplectic mapping option (called `MVS` in the input files). We used step sizes varying from 2 to 400 d. Secondly, we used the NBI package, which contains a 14th-order Cowell–Störmer method with modifications by the UCLA research group led by William Newman (Grazier et al. 1995, 1996; Varadi et al. 2003).¹ NBI has been shown to have relative truncation errors below the double precision machine epsilon (about 2×10^{-16}) when more than 1000 steps per orbit are used and the orbital eccentricity is less than 0.5.² More precisely, if the largest component of the phase-space vector of the solution at time t has absolute value M , then the local errors per step of each of the components are all less than $2 \times 10^{-16}M$. Note that this means that the component-by-component relative error can be significantly greater than the machine precision for components of the solution that are significantly less than M , but all components have errors relative to M which are smaller than the machine precision. Furthermore, the authors of NBI have gone through great pains to ensure that the round-off error is unbiased. We used a 4-d time-step for all NBI integrations, which gives more than 1000 time-steps per Jupiter orbit. We have verified the above ‘exact to double precision’ property by comparison against quadruple precision integrations described below. Note that such an integration is symplectic by default since it is equivalent to the locally exact solution rounded to machine precision. Furthermore, except for the possibility of having the same property with a larger time-step, this is practically as good an integration as is possible using double precision. In our 200-Myr integrations, NBI always had relative energy errors and angular momentum errors of less than 2×10^{-11} , with an average of about 2×10^{-12} .

Our third integrator was the TAYLOR 1.4 package (Jorba & Zou 2005). TAYLOR 1.4 is a recent and impressive advance in integration technology. It is a general-purpose, off-the-shelf integrator which utilizes automatic differentiation to compute arbitrary order Taylor series expansions of the right-hand side of the ordinary differential equation (ODE). TAYLOR 1.4 automatically adjusts the order and step size at each integration step in an effort to minimize truncation error, and utilizes Horner’s rule in the evaluation of the TAYLOR series to minimize round-off error. As the authors note, integration accuracy is gained more efficiently by increasing the order of the integration than by decreasing the time-step, since the accuracy increases exponentially with the order but only polynomially in the time-step. Although TAYLOR 1.4 allows the user to specify a constant order and time-step, we chose to allow it to use variable order and time-step while providing it with a requested relative error tolerance equal to 1/1000 of the machine precision, in order to produce solutions which were exact to within round-off error. We found that TAYLOR 1.4 typically used 27th order with about a 220-d time-step, although orders of 26th and 28th were observed, and time-steps varied between about 200 and 240 d. We allowed TAYLOR 1.4 to choose its order and time-step automatically, with the only constraint being that the

tolerance was set three orders of magnitude below machine precision. The fact that the solution is exact to machine precision over such a long time-step guarantees that accumulated round off is by far the smallest in the TAYLOR 1.4 integrations. Furthermore, Taylor series integrators are extremely stable when applied to non-stiff problems, with the radius of convergence increasing linearly with integration order, and in our case the time-step is well within the radius of convergence (Barrio, Blesa & Lara 2005). Finally, TAYLOR 1.4 allows the user to specify the machine arithmetic to use, including software arithmetics. Out-of-the-box, TAYLOR 1.4 supports the use of IEEE 754 DOUBLE precision (64 bit representation with a 53 bit mantissa), Intel extended precision [80 bit representation with a 64 bit mantissa, giving a machine precision of about 10^{-19} , accessible as LONG DOUBLE when using GCC (GNU Compiler Collection) on an Intel machine], the DOUBLEDDOUBLE data type³ which provides software quadruple precision in C++, and the GNU Multiple Precision Library, which allows arbitrary precision floating point numbers in C++. Most of our integrations using TAYLOR 1.4 used Intel extended precision, which is almost as fast as double precision and gives about 19 decimal digits of accuracy. Over our 200-Myr integrations using Intel extended precision, TAYLOR 1.4 typically had relative energy errors of less than 8×10^{-14} ; the worst relative energy error observed in any of our integrations was 2×10^{-13} . Integrations began with the Solar system’s barycentre at the origin with zero velocity. After 200 Myr the barycentre drifted a maximum of 3×10^{-10} au, while the z component of the angular momentum was always conserved to a relative accuracy better than 3×10^{-14} . We also performed a suite of quadruple precision integrations, in which energy and angular momentum were each conserved to at least 26 significant digits over 200 Myr.

Now we analyse the error growth as a function of time for our non-symplectic integrators, applied to a non-chaotic IC. One consequence of having a solution whose numerical error is dominated by unbiased round off (i.e. exact to machine precision) is that when integrating a non-chaotic system, the total phase-space error grows polynomially as $t^{1.5}$. If the local error is biased (either by biased round off, or due to truncation errors in the integration scheme), then the total phase-space error grows as t^2 . (This is assuming that the integrator is not inherently symplectic, as is the case with both NBI and TAYLOR 1.4.) This is known as Brouwer’s law (Brouwer 1937). As noted above, we chose a time-step for NBI such that its integration is dominated by unbiased round off. We tested TAYLOR 1.4 in Intel extended precision for similar properties by integrating the system of Jovian planets for 200 Myr using various integration tolerances up to and beyond the machine precision of 10^{-19} , and compared these integrations to a TAYLOR 1.4 integration that used quadruple precision. In Fig. 1, we plot the phase-space separation between the quadruple precision integration and several integrations using Intel extended precision. We see that when the relative integration tolerance is set above the machine precision, the error grows as t^2 and is therefore truncation dominated. However, when the tolerance is set to 10^{-22} (about a factor of 1000 below the machine precision), the error grows as $t^{1.5}$, and is therefore dominated by unbiased round off. This is consistent with TAYLOR 1.4 producing results that are exact in Intel extended precision when given a local relative error tolerance of 10^{-22} , just as NBI produces exact results in double precision when used with 1000 or more time-steps per orbit. We see that after 200 Myr, the errors in the positions of the planets are of order 10^{-5} au (in the case of non-chaotic ICs). This

¹ NBI is available at <http://astrobiology.ucla.edu/~varadi/NBI/NBI.html>, or by searching the web for ‘NBI VARADI’.

² Note that these properties may be attainable with a larger time-step (Goldstein 1996; Grazier 1997), but we did not test any other values of time-step.

³ Developed by K. Briggs (<http://keithbriggs.info/doubledouble.html>).

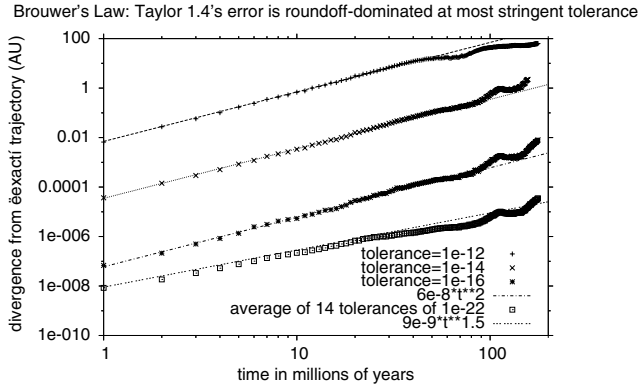


Figure 1. TAYLOR 1.4 satisfies Brouwer’s law: when local tolerance is set above machine precision of 10^{-19} , phase-space error grows as t^2 due to biased truncation errors (upper three curves). However, with tolerance set well below the machine precision, its result is exact (i.e. correctly rounded) to machine precision, so that phase-space error grows only as $t^{1.5}$ (lowest curve).

translates into a phase error, or equivalently an observational error, of substantially less than 1 arcmin. A comparison of our Fig. 1 with fig. 2 of Grazier et al. (1999) at their 200 Myr mark also demonstrates that TAYLOR 1.4 using Intel extended precision provides about three extra digits of precision over NBI using double precision, as would be expected when comparing 19-digit and 16-digit integrations. As we show later (Fig. 7), the differences in orbital elements are even smaller.

For comparison, we briefly mention the run-times of the integration algorithms. All timings are for a 2.8 GHz Pentium 4 processor. As we shall see later, the largest time-step for which the MERCURY 6.2 integrations agreed with the others was 8 d; a 16-d time-step was almost as good. Thus we compare the Wisdom–Holman mapping with time-steps of 16 and 8 d to NBI with a 4-d time-step, and TAYLOR 1.4. In addition to the TAYLOR 1.4 extended precision (LONG DOUBLE) timings used in this paper, we present its timings for standard IEEE 754 DOUBLE precision, for comparison to the other DOUBLE precision integrations. Table 1 presents the results. We found that the total run-time was linearly proportional to the inverse of the time-step, as would be expected. We note several observations. First, TAYLOR 1.4 is not competitive in terms of efficiency. However, note that TAYLOR 1.4 is a ‘proof-of-concept’ software package for general-purpose integration of any system of ODEs, and it currently generates code that can be quite inefficient. A carefully hand-coded TAYLOR series integrator for Solar system integrations is far more efficient, and can be competitive with the above codes (Carles Simo, personal communication). Secondly, Wisdom–Holman with an 8-d time-step is the fastest case among the integrations we tested that showed complete convergence. Thirdly, Wisdom–Holman with a 4-d time-step (51 h, not shown in the table) is slower than NBI with a 4-d time-step. Finally, although we did not test NBI for convergence at time-steps less stringent than 4 d, it is capable of maintaining the lead in

being more efficient than Wisdom–Holman with larger time-steps (Goldstein 1996; Grazier 1997).

We will not directly measure the Lyapunov time in this paper, since it is difficult to create an objective measure of the Lyapunov time over a finite time interval. Formally, the Lyapunov time is only defined over an infinite time interval. In practical terms, the divergence is almost always polynomial for some non-trivial duration before the exponential divergence emerges, and it is difficult to pinpoint the changeover objectively. However, when plotting the distance between two nearby trajectories as a function of time, it is usually evident by visual inspection whether or not exponential divergence has occurred by the end of the simulation. Thus we will plot the actual divergence between two numerical trajectories initially differing by perturbing the position of Uranus by 10^{-14} au (about 1.5 mm) in the z direction. We will call these pairs of trajectories ‘siblings’. In the cases where we see only polynomial divergence between siblings over a 200-Myr integration, we will abuse terminology and call these systems ‘regular’, ‘near-integrable’ or ‘non-chaotic’, although formally all we have shown is that the Lyapunov time is longer than can be detected in a 200-Myr integration.

As a prelude to our main results, we first crudely reproduce the results of Murray & Holman (1999). Murray & Holman performed a survey in which the semimajor axis of Uranus a_U was varied around its actual value, plotting the measured Lyapunov time as a function of a_U . Broadly, they found that below $a_U \approx 19.18$ au, the Lyapunov time was substantially less than 10^7 yr, sometimes as small as 10^5 yr; in the range $a_U \approx 19.20$ – 19.22 au, the Lyapunov time fluctuated between about 1 and 10 Myr, interspersed with cases in which the motion was regular; near $a_U = 19.24$ au it was uniformly regular; near $a_U = 19.26$ au there was a tightly packed region of both chaotic and regular orbits and near $a_U = 19.28$ au the motion was again uniformly regular. We have reproduced this survey using quadruple precision integrations, using a very coarse grid in a_U due to computing constraints. (On a 2.8 GHz Intel Pentium 4, a quadruple precision integration using TAYLOR 1.4 proceeds roughly at 100 Myr per month of CPU time.) Fig. 2 displays the distance between siblings for various values of a_U . Although we were not able to perform the survey using a finer grid in a_U due to the computational expense, we see that in broad outline we obtain results similar to Murray & Holman. In Fig. 3, we repeat the same survey using Intel extended precision. We see that the results are qualitatively identical, demonstrating that 19 digits of precision (which requires about 1/20 of the CPU time of quadruple precision) gives qualitatively identical, and quantitatively very similar, results. Henceforth in this paper, all TAYLOR 1.4 integrations are performed using Intel extended precision, with the relative local error tolerance set to 10^{-22} .

3 RESULTS

3.1 Corroborating previous results

As an early step, the author obtained from Murray and Holman their ICs used in Murray & Holman (1999), and verified using accurate

Table 1. Run-times for integrating the five-body system for 200 Myr on a 2.8 GHz Pentium 4 for MERCURY 6.2 (using the Wisdom–Holman integrator – ‘WH’) with time-steps of 16, 8 and 4 d; for NBI with a 4-d time-step and TAYLOR 1.4 – ‘T’, in DOUBLE, LONG DOUBLE and DOUBLEDDOUBLE (i.e. quad) precision.

Integrator	WH 16 d	WH 8 d	WH 4 d	NBI	T DOUBLE	T LONG DOUBLE	T DOUBLEDDOUBLE
Time (h)	13	26	51	40	100	150 (1 week)	1500 (2 months)

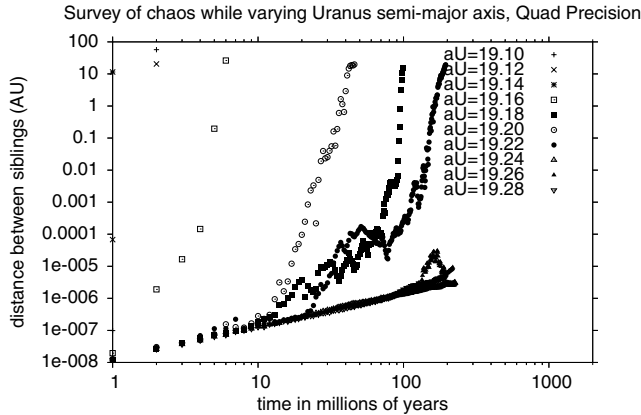


Figure 2. Murray & Holman (1999) in quadruple precision.

integrations that their system was chaotic. The author then obtained from P. Sharp the ICs used by Grazier et al. (2005), and verified that their system was regular, at least over a 200-Myr time-span. The author then spent significant time eliminating several possible reasons for the discrepancy, such as incorrect ICs, incorrect deletion of the inner planets etc. The author also integrated from one set of ICs to the other (having along the way to account for the fact that they were in different coordinate systems), and finally found that the systems agreed with each other to a few parts in 10^7 when integrated to the same epoch. After some time it became apparent that neither group of authors had made any obvious errors. The conclusion seemed to be that both systems nominally represented the outer Solar system to within observational error, but one was chaotic and one was not.

3.2 Ephemeris initial conditions drawn at different times

It is reasonable to make the assumption that either our Solar system is chaotic, or it is not. It cannot be both. This appears to be the assumption that most practitioners make when measuring ‘the’ Lyapunov time of our Solar system. Although this is probably a reasonable assumption, it does not follow that all ICs drawn from an ephemeris are equivalent. The most recent ephemeris published by JPL is DE405 (Standish 1998). It is based upon hundreds of thousands of observations, all of which have finite error. Thus, the ephemeris does not represent the exact Solar system. For the outer planets, the best match of DE405 to the observations yields residual errors of a few parts in 10^7 (Morrison & Evans 1998; Standish 1998). The masses of the planets are also known to only a few parts in 10^7 . Note that the product GM_i for each planet i is known to much higher accuracy than either G or M_i alone; however, the initial positions and velocities are still only known to about seven digits, and these are the main focus of this paper. It is possible that within these error bounds there exist different solutions with different Lyapunov times. In particular, it may be possible that some solutions display chaos on a 200-Myr time-scale, while others do not.

To test this hypothesis, we drew 21 sets of ICs from DE405, at 30-d intervals starting at Julian Date 244 8235 (1990 December 9.5). We represent each of our 21 sets of ICs using a three-digit numeral, 000, 030, 060, . . . , 570, 600, representing the number of days after JD 244 8235 at which the IC is drawn. We chose a 2-yr total interval across which to draw our ICs in order to ensure a reasonable sample of inner-planet positions before deleting the inner planets (a Martian year is about 2 Earth years). We drew the ICs by

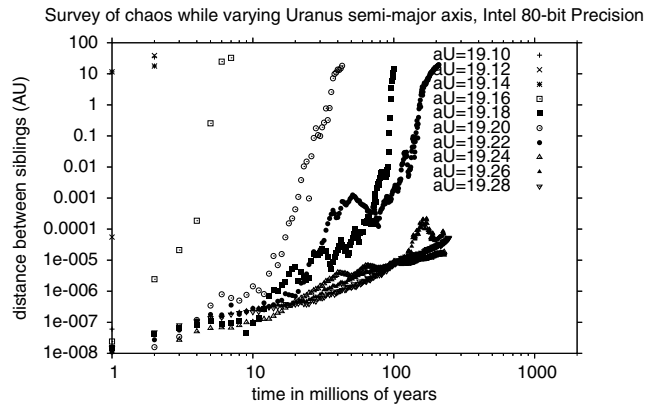


Figure 3. Murray & Holman (1999) in LONG DOUBLE.

taking the output of the program TESTEPH.F, which is included with the DE405 ephemeris. The output of TESTEPH.F is rounded to seven digits, since no more digits are justifiable.⁴ As described above, we augment the mass of the Sun with that of the inner planets and augment the Sun’s position and linear momentum to match that of the inner Solar system. For each of the 21 ICs, we generate a ‘sibling’ IC which is offset by 10^{-14} au (1.5 mm). We then integrate both of them for 200 Myr, and measure the distance between them at 1-Myr intervals. To ensure that our results are not integrator- or time-step dependent, we perform each integration in several ways: first, with the Wisdom–Holman symplectic mapping included with MERCURY 6.2 (Chambers 1999) with time-steps of 400, 200, 100, 50, 32, 16, 8, 4 and 2 d; secondly, with NBI with a time-step of 4 d and thirdly, with TAYLOR 1.4 in Intel extended precision with a relative error tolerance of 10^{-22} . Results for the Wisdom–Holman integrations with larger time-steps are displayed in Fig. 4. Several key observations present themselves. First, when comparing across the 21 sets of ICs, there is remarkable disagreement about whether or not the outer Solar system displays exponential divergence. This will be discussed further below, using more accurate integrations. Looking at an individual graph, but across time-steps, we note that there are very few cases (e.g. $t = 150, 330, 420$) in which there is universal agreement between all four time-steps that divergence is polynomial. There are also only a few cases that universally agree that the divergence is exponential. In most cases, there is substantial disagreement across time-steps whether a particular IC admits chaos. This is consistent with the observation of Newman et al. (2000). However, in contrast to Newman et al. (2000), we note that the ‘switch’ from chaos to non-chaos is not always monotonic in time-step. For example, for system 000, time-steps of 400 and 50 d admit chaos, while the ‘in-between’ time-steps of 200 and 100 d do not. For system 180, time-steps of 400 and 200 d display non-chaos, while for 100 and 50 d time-steps, chaos is apparent; this is precisely opposite to what one would expect if large time-steps were injecting chaos into the system. As we shall see later in the paper (Table 2), there appears also to be no observable correlation between the time-step and the percentage of ICs that admit chaos. Thus we hypothesize that the discrepancy across time-steps is due more to perturbations in the ICs and our use of only low-order symplectic correctors (Wisdom

⁴ Although this is probably not the best way to uniformly sample ICs from within the error volume representing the error in the observations, it does represent a reasonable way to reproduce how users of DE405, taking ICs from DE405 to seven digits, get their samples.

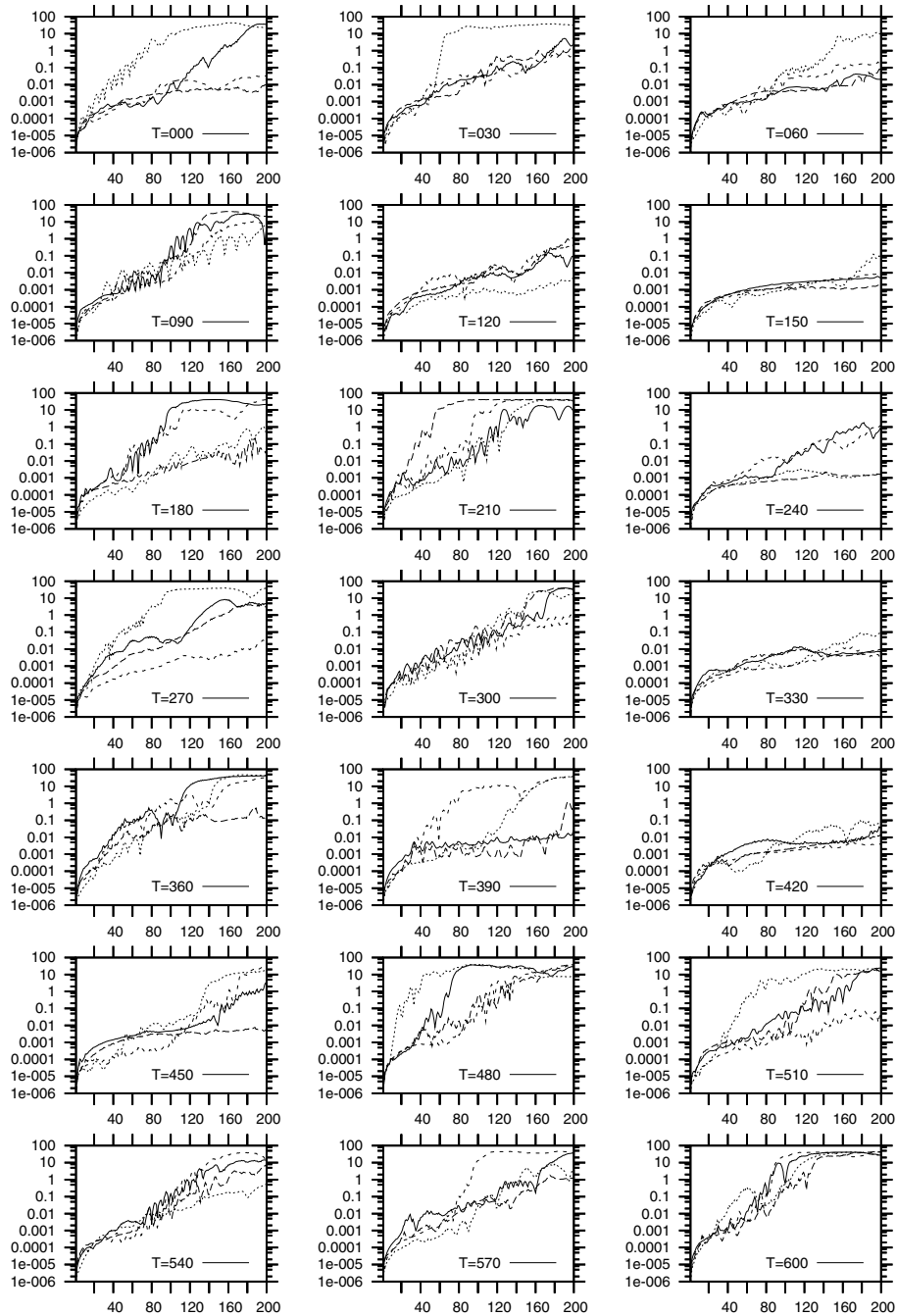


Figure 4. Distance in astronomical unit (au) between ‘sibling’ trajectories as a function of time for 21 sets of ICs drawn from DE405 at 30-d intervals. Each ‘postage stamp’ graph depicts one IC, integrated with four different time-steps. Siblings are integrated with the Wisdom–Holman symplectic map with time-steps: 50 d (solid line), 100 d (long dash), 200 d (short dash) and 400 d (dotted). For any given plot, note disagreement across time-steps, and that the switch between chaos and regularity is not always monotonic with time-step.

et al. 1996; Chambers 1999), than it is due to unreliable integration at large time-steps. Supporting this hypothesis would require us to reperform these experiments using a ‘warm-up’ procedure (Saha & Tremaine 1992), or higher order symplectic correctors (Wisdom et al. 1996; Wisdom 2006). This is a possible direction for future research.

Figs 5 and 6 plot the divergence between sibling trajectories for all 21 ICs, as integrated by more accurate integrations showing convergence: NBI, the Wisdom–Holman mappings with time-steps of 8 and 4 d and TAYLOR 1.4. Wisdom–Holman with 2-d time-steps

agreed with these curves, but are omitted to reduce clutter; Wisdom–Holman with a time-step of 16 d also showed good agreement in all but two cases. Both figures are identical except that Fig. 5 uses a log–linear scale, while Fig. 6 uses a log–log scale; different features are visible using the different scales. At least two observations present themselves from these figures. First, if one looks at the system corresponding to any single IC, there is usually good agreement between the integrations as to the future divergence between the sibling trajectories of that particular case. This demonstrates that convergence has occurred and makes it unlikely that the results are integrator

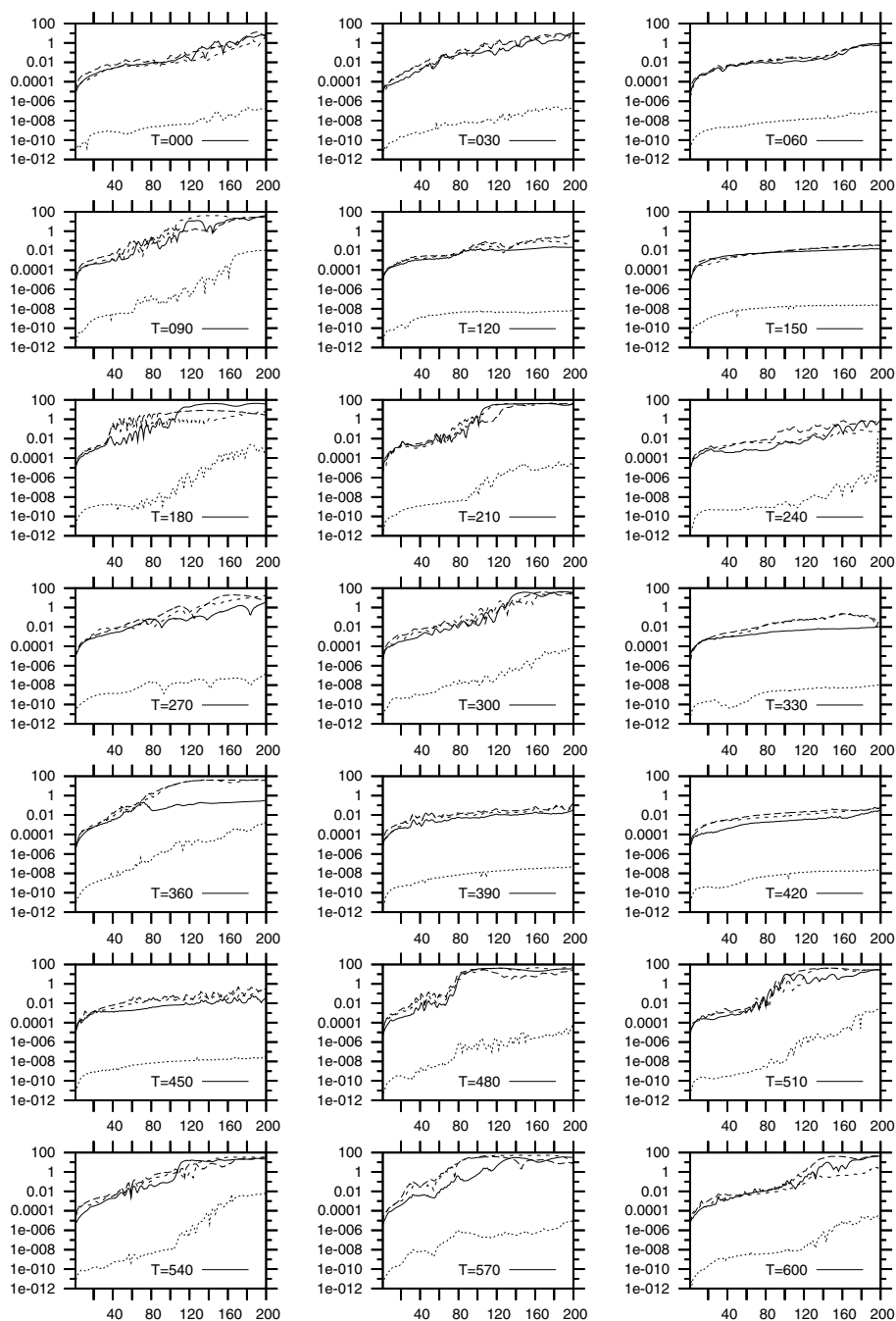


Figure 5. Similar to previous figure, but more accurate integrations. NBI: solid lines; Wisdom–Holman: dashed lines with $dt = 8$ d (long dash), 4 d (short dash); dotted lines (TAYLOR 1.4) are shifted below others because TAYLOR 1.4 is more accurate. For any given IC, there is good agreement between the shapes of the curves, indicating agreement on the existence (or lack) of chaos. (Divergence saturates at ≈ 100 au.)

dependent. Secondly, looking across cases, it appears that the future of the outer Solar system over the next 200 Myr is quite uncertain, varying from nearly integrable to chaotic with a Lyapunov time of order 10 Myr or less. This is quite a startlingly diverse array of possible outcomes, considering that the ICs for these systems are all drawn from the same ephemeris, all less than 2 yr apart, and presumably differing from each other by only a few parts in 10^7 . The author has, in fact, verified that several of the ICs, when all integrated up to the same epoch in the vicinity of 1991, agree with each other to a few parts in 10^7 .

Figs 5 and 6 demonstrate that in the chaotic cases, the siblings can have their respective planets on opposite sides of the Solar system after 200 Myr. However, Fig. 7 demonstrates that changes in the orbital elements are much less drastic, demonstrating that the Solar system is practically stable over a 200-Myr time-scale even when it is chaotic.

3.3 Explicitly perturbed initial conditions

Following Murray & Holman (1999), we performed several surveys in which we perturbed the semimajor axis a_U of Uranus from its

Table 2. The percentage of ICs drawn from DE405 that admit chaos. Column labels: ‘*C*’ is the cut-off described in the text; ‘*dt*’ is the time-step; ‘/10’ means out of the 10 ICs drawn at 10-yr intervals from 1900 to 1990; ‘/21’ means out of the 21 ICs drawn at 30-d intervals starting at 1990; ‘Total’ is the sum of the previous two columns; ‘Per cent’ is the percentage of systems out of the 31 that display chaos according to the cut-off.

<i>dt</i>	<i>C</i> = 1				<i>C</i> = 0.1			
	/10	/21	Total	Per cent	/10	/21	Total	Per cent
400	7	14	21	67.7	9	16	25	80.6
200	7	11	18	58.1	8	15	23	74.2
100	6	11	17	54.8	8	13	21	67.7
050	6	14	20	64.5	8	15	23	74.2
032	7	10	17	54.8	9	15	24	77.4
016	7	14	21	67.7	8	16	24	77.4
008	8	13	21	67.7	8	14	22	71.0
004	8	13	21	67.7	8	18	26	83.9
002	8	13	21	67.7	8	15	23	74.2

current value, but kept all other ICs constant. We used all three previously mentioned integrators: Wisdom–Holman with time-steps of 4 and 8 d; NBI and TAYLOR 1.4. The IC was the default one from the file BIG.IN included with MERCURY 6.2 (Chambers 1999), which according to the documentation is from JD 245 1000.5. The inner planets were deleted, with their mass and momentum augmenting the Sun’s as described elsewhere in this paper. We completed surveys in which a_U was changed in steps of 2×10^{-k} au, for $k = 6, 7, 8$, which corresponds to $\Delta a_U/a_U$ in steps of $10^{-(k+1)}$. We went 10 steps in each direction for each value of k . For each step, we generated a ‘sibling’ IC by randomly perturbing the positions of all planets by an amount bounded by 10^{-14} au.⁵ We then integrated both for 200 Myr, and plotted the distance between them as a function of time. For $k = 7, 8$, there was no significant difference between any of the integrations. That is, all siblings at all steps had virtually identical divergences when changing a_U in 10 steps of $2 \times 10^{-(7,8)}$ au, for a total change of 2×10^{-6} au. This corresponds to $\Delta a_U/a_U$ stepped by $10^{-(8,9)}$ for a total change in $\Delta a_U/a_U$ of 10^{-7} in each direction. However, for $k = 6$, some of the steps showed chaos while others did not. The change was not monotonic: over the 21 steps (10 in either direction plus the ‘baseline’ case), there were three ‘switches’ between chaos and stability.

Fig. 8 plots two of these 21 systems. The value of $\Delta a_U/a_U$ differs between the two systems by one part in 10^7 . One of the systems appears chaotic, and the other does not, over a 200-Myr time-span. The non-chaotic one has a semimajor axis of $a_U + 2 \times 10^{-6}$ au, while the chaotic one has semimajor axis $a_U + 4 \times 10^{-6}$ au. All other ICs in the two systems are identical. To ensure that the result is not integrator dependent, we have repeated the integrations with the Wisdom–Holman mapping included in MERCURY 6.2 with time-steps of 8 and 4 d; and with NBI with a time-step of 4 d. As can be seen, all the integrations agree quite well with one another. Note that the TAYLOR 1.4 integrations provide three extra digits of precision, and so the curves for TAYLOR 1.4 are displaced about three orders of magnitude below the curves computed in double precision. Otherwise the shapes of the curves are virtually identical. We note that the chaotic one has a Lyapunov time of about 12 Myr, while the

⁵ Note that, due to a programming inconsistency on the part of the author, this is different from the perturbations used to generate siblings in the rest of the paper. However, we do not expect the precise form of these mm-scale perturbations to affect the results.

regular one has the sibling trajectories separating from each other polynomially in time as $t^{1.5}$.

3.4 Accurate integrations over the age of the Solar system

The author has reported related results for integrations lasting 10^9 yr (Hayes 2007). The essential conclusion is the same, in that even after 10^9 yr, there remain some ICs (about 10 per cent) that show no evidence of chaos, although some of the ICs appearing as regular over 200 Myr develop exponential divergence later.

Fig. 9 displays the sibling divergence over 5×10^9 yr of the ‘canonical’ IC used by DE405 (JED 244 0400.5, 1969 June 28). As we can see, this IC shows little evidence of chaos for about the first 1.5 Gyr, and then develops slow exponential divergence with a Lyapunov time between about 200 and 400 Myr. The individual planet each shows similarly shaped divergence curves (not shown), with the magnitude of divergence increasing with orbital radius. After 5 Gyr, the uncertainty in Jupiter’s position for this IC is less than 1 au, while the uncertainty in Neptune’s position is about 9 au. Thus, there is a non-negligible chance that, if the Solar system lies close enough to the ‘canonical’ IC of DE405, we can know within about 10^{-15} ° where each outer planet will be in its orbit when the Sun ends its main-sequence lifetime and becomes a red giant. Note that the levelling-off that starts at about the 4 Gyr mark is not saturation (which occurs closer to 100 au separation, while the separation at 5 Gyr here is less than 10 au); the outer Solar system instead seems to be entering again into a period of polynomial (non-chaotic) divergence.

3.5 Percentage of initial conditions displaying chaos

Observing the distance between sibling trajectories in Figs 5 and 6 at the 200 Myr mark, we can reasonably simplify the distinction between chaotic and regular trajectories. By choosing a cut-off distance C and restricting our view to the various double-precision integrations, we can claim that siblings differing by less than C after 200 Myr are regular (in the sense of having no observable Lyapunov exponent), while those differing by more than C are chaotic with a measurable positive Lyapunov exponent. Table 2 lists the number of systems that are chaotic by the above definition, as a function of time-step and cut-off. In addition to the 21-sample group of ICs displayed in Figs 5 and 6, we also drew a second sample group of 10 samples, spaced at 10-yr intervals from 1900 to 1990. Since the TESTEPH.F program included in DE405 provides only seven digits of precision (corresponding to the accuracy to which the positions are known), taking ICs from DE405 at different times effectively takes ICs from different exact orbits, differing from each other by as much as one part in 10^7 . (As noted in a previous footnote, this method of sampling may not ideally represent an unbiased sample from the observational error volume; instead, it is an unbiased sample from the set of seven-digit-rounded ICs drawn from DE405.) We make several observations. First, the fraction of sampled systems that are chaotic by this simple definition is roughly about (70 ± 10) per cent, and is relatively independent of both the time-step and the two sample groups (30-d versus 10-yr samples), although it of course increases as we decrease the cut-off. Recall that for a given IC, different step sizes can give different results, so that which systems are chaotic changes as the time-step changes. However, here we measure only the number of chaotic systems as a function of time-step. If chaos were being ‘injected’ into the system by the integrator, we would expect that the number of systems displaying chaos

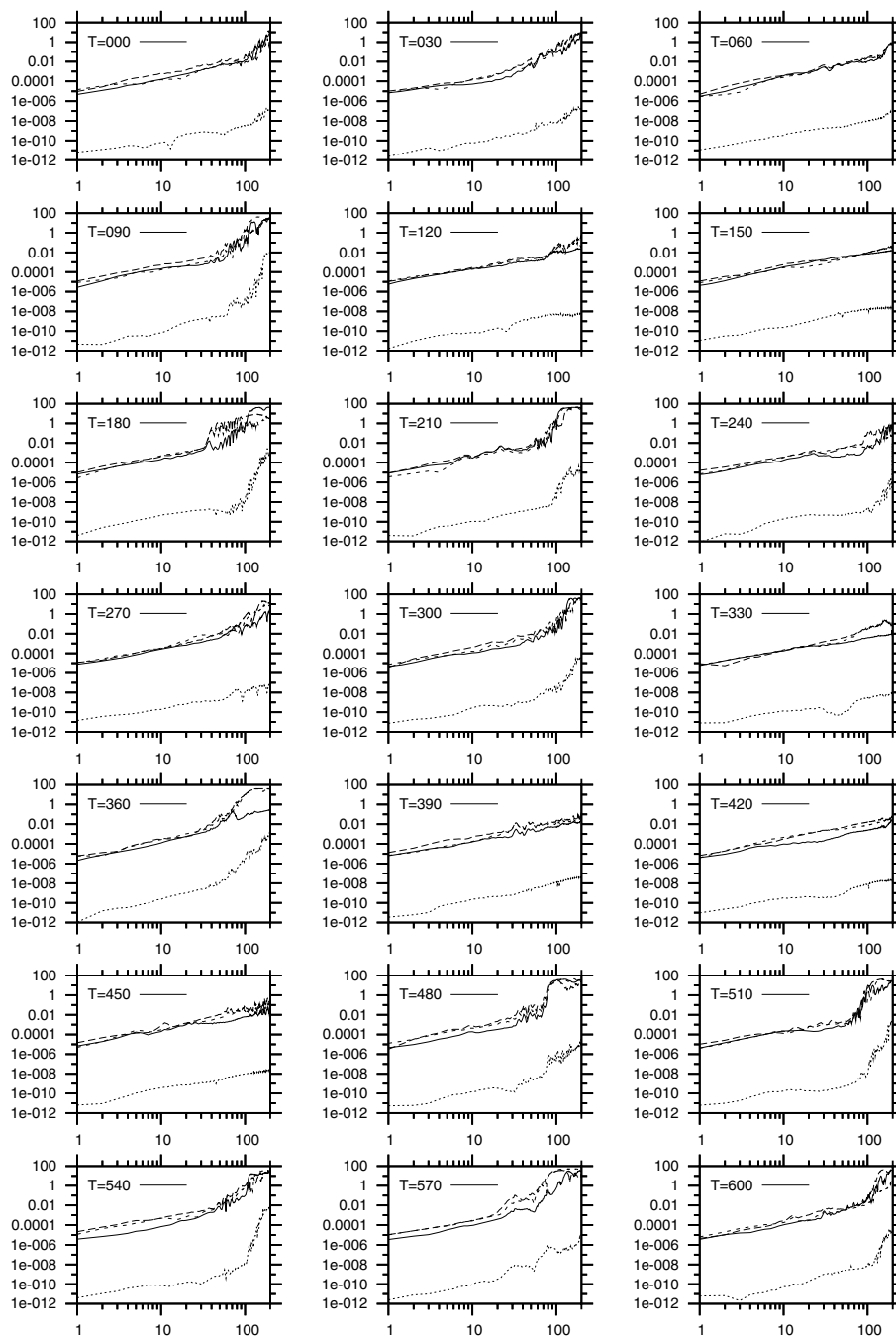


Figure 6. Curves identical to the previous figure, but plotted on a log–log scale, which depicts polynomial divergence as a straight line.

should increase with increasing time-step. However, this is not observed. A possible interpretation of this is that even a 400-d time-step reliably determines whether some system is chaotic, but the system is slightly different for each time-step due to the IC perturbation introduced by the symplectic integration (Saha & Tremaine 1992; Wisdom et al. 1996). Verifying this would require us to implement a ‘warm-up’ procedure (Saha & Tremaine 1992) or higher order symplectic correctors than are included with MERCURY 6.2 (Chambers 1999), which we have not done. However, the fact that the fraction of systems displaying chaos is independent of time-step argues against the ‘chaos is injected by the integrator’ hypothesis, at least for the time-steps used in this paper.

3.6 Chaos in the inner Solar system is robust

Varadi et al. (2003) performed a 207-Myr integration of the entire Solar system, including some non-Newtonian effects and a highly tuned approximation to the effects of the Moon, and placed a lower bound of 30 Myr on the Lyapunov time of the outer Solar system. However, they still saw chaos in the inner Solar system. To test the robustness of chaos in the inner Solar system, we performed several integrations of eight planets (Mercury through Neptune) using the Wisdom–Holman mapping with time-steps of 8, 4, 2, 1 and 0.5 d. We treated the Earth–Moon system as a single body. To ensure that chaos in the outer Solar system did not ‘infect’ the inner

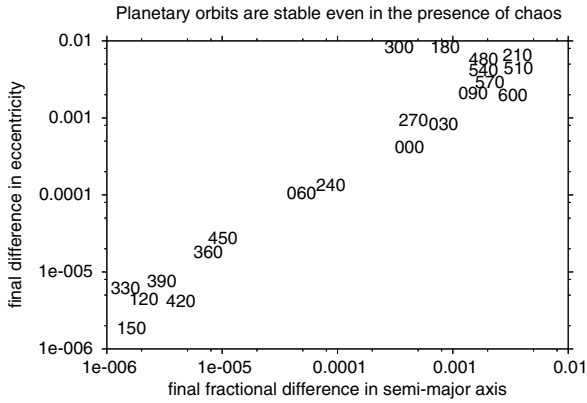


Figure 7. The final difference at the 200 Myr mark between siblings, in semimajor axis and eccentricity, for the 21 cases depicted in the previous figures. The integrator was NBI. Eccentricity difference is the Euclidean distance between siblings in the four-dimensional space consisting of the four orbital eccentricities. Semimajor axis difference is the Euclidean distance between siblings in the four-dimensional space consisting of the four $\Delta a/a$ values. Some values have been moved slightly for textual clarity, but in no case by more than the width or height of a character.

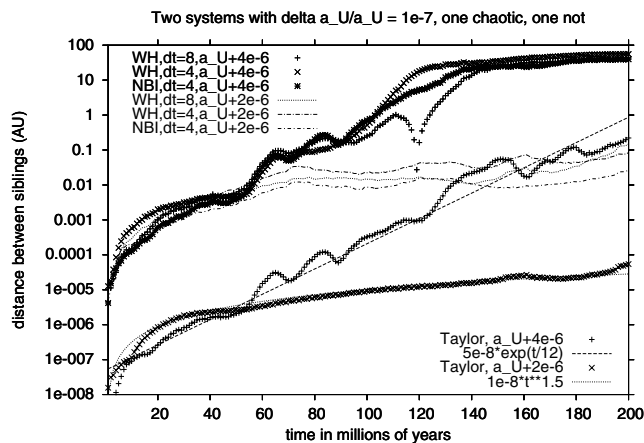


Figure 8. Two systems, both using ICs within the error bounds of the best-known positions for the outer planets. Both have identical ICs except for the semimajor axis a_U of Uranus, which differs between the two systems by 10^{-7} in $\Delta a_U/a_U$. One admits chaos, while the other does not. The ‘upper’ six curves (all starting with sibling distances near 10^{-5}) are all double-precision integrations, two using Wisdom–Holman with time-steps of 4 and 8 d, and one using NBI. Of the six, the three plotted with points are the chaotic trajectory and the three plotted with lines are the non-chaotic trajectory. The ‘lower’ two curves (starting with sibling distances near 10^{-8}) are integrated in extended precision with TAYLOR 1.4. The chaotic one fits an exponential curve with a Lyapunov time of about 12 Myr, while the non-chaotic one has the two trajectories separating approximately as $t^{1.5}$.

Solar system, we used only those DE405 ICs from Figs 5 and 6 for which the outer Solar system was regular over 200 Myr. We then integrated the system until chaos appeared. In all cases, even though the outer Solar system was regular, the inner Solar system displayed chaos over a short time-scale such that information about the inner planetary positions was lost within about 20–50 Myr. Thus, unlike the outer Solar system, we observe that chaos in the inner Solar system is robust.

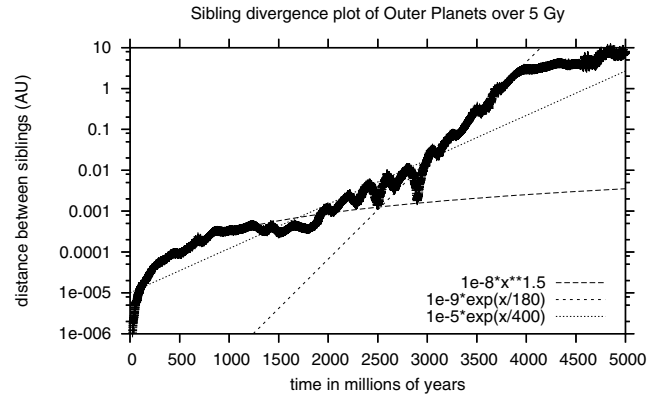


Figure 9. Sibling divergence over 5 Gyr of the canonical IC of DE405, integrated using TAYLOR 1.4.

4 DISCUSSION

We conclude that perturbations in the ICs of the outer planets as small as one part in 10^7 can change the behaviour from regular to chaotic, and back, when measured over a time-span of 200 Myr. We believe this is the first demonstration of the ‘switch’ from chaos to near-integrability with such a small perturbation of the ICs. Since our knowledge of the orbital positions of the outer planets is comparable to one part in 10^7 , it follows that, even if our simplistic physical model accounting only for Newtonian gravity were the correct model, it would be impossible at present to determine the Lyapunov time of the system of Jovian planets. Furthermore, it implies that an IC with seven digits of precision (which is all an ephemeris can justifiably provide) can randomly lie on a chaotic or non-chaotic trajectory. Since our results converge in the limit of small time-step for the Wisdom–Holman mapping, and the converged results also agree with two very different high-accuracy integrations, and finally since the high-accuracy integrations in turn agree very well with quadruple-precision integrations, we believe that the results in this paper are substantially free of significant numerical artefact.

Guzzo (2005) corroborates the existence of a large web of three-body resonances in the outer Solar system, and finds that their placement is consistent with Murray & Holman’s (1999) theory. Guzzo used his own fourth-order symplectic integrator (Guzzo 2001), and performed what appear to be reasonable convergence tests to verify the robustness of his main results. Thus, Murray & Holman’s theory appears to explain the existence and placement of three-planet resonances. Furthermore, chaotic regions in Hamiltonian systems are usually densely packed with both chaotic and regular orbits (Lichtenberg & Leiberman 1992). This paper corroborates the observation of densely packed regular and chaotic orbits, at a scale previously unexplored for the system of Jovian planets.

As discussed in the text relating to Fig. 8, we performed surveys across the semimajor axis a_U of Uranus in steps of 2×10^{-k} au for $k = 6, 7, 8$. We found that, around the current best-estimate value of a_U , perturbations smaller than 2×10^{-6} au had no effect on the existence of chaos. However, this does not imply that perturbations of this small cannot have an effect; it simply means that the ‘border’ between chaos and regularity is not within 2×10^{-6} au of the current best estimate of a_U . However, it is clear that the border between chaos and regularity is between the two systems depicted in Fig. 8, which differ from each other in a_U by 2×10^{-6} au. Although a survey across a_U for values between those two systems may not be very relevant from a physical standpoint, it might be very interesting from a dynamical systems and chaos perspective to probe

the structure of the border between chaos and regularity. In particular, it may be interesting to see if the border itself has some sort of fractal structure (Mandelbrot 1982). Such chaotic structure has already been observed in the circular restricted three-body problem (Murison 1989).

Newman et al. (2000) gave a compelling demonstration that the Wisdom–Holman symplectic mapping with too large a time-step could introduce chaos into a near-integrable system by first showing that they could reproduce the chaos with a 400-d time-step, and then showing that the integration converged to being regular with a time-step of about 50 d or less. Our results appear to hint that an even smaller time-step may be required: our curves depicting divergence-of-nearby-orbits did not fully converge until the time-step was 8 d or less. On the other hand, the symplectic integrators produce solutions that effectively integrate a system with slightly perturbed ICs, although these perturbations decrease with decreasing time-step (Saha & Tremaine 1992; Wisdom et al. 1996). Our Fig. 4 demonstrates that the behaviour does not always ‘switch’ monotonically in time-step from chaotic to non-chaotic as observed by Newman et al. (2000); Table 2 also hints that the ‘amount’ of chaos does not appear to increase with increasing time-step. An alternate interpretation is that even a 400-d time-step accurately integrates an orbit, but not the orbit that we chose. In particular, it may accurately integrate an orbit whose IC is perturbed slightly from the one we chose, and an appropriate correction may allow us to recover the correct orbit using an integration with much larger time-step (Saha & Tremaine 1992; Wisdom et al. 1996). However, the symplectic correctors in MERCURY 6.2 are clearly not good enough to perform this recovery at a 400-d time-step; better correctors (Wisdom 2006) or warm-up (Saha & Tremaine 1992) may be able to achieve this.

The convergence of our results at time-steps of 8 d or less, as well as the agreement with two different non-symplectic integrators (including the one used by Newman et al.), indicate that the IC perturbations described by Saha & Tremaine (1992) and Wisdom et al. (1996) are negligible in our smaller time-step cases. Thus, using ‘warm-up’ (Saha & Tremaine 1992) or higher order symplectic correctors will not substantially alter our conclusions, although they might allow the same conclusions to be drawn using larger time-steps.

With the exception of the results plotted in Fig. 9, all of our simulations had a duration of 200 Myr. All of them display an initial period of polynomial divergence, before the appearance of exponential divergence (if any). However, the duration of initial polynomial divergence differs greatly across systems, and has been observed by others (Lecar et al. 2001) to last significantly longer than 200 Myr; Grazier et al. (2005) observed it to last the entire duration of their 800-Myr simulation. It would be interesting to create a table like Table 2, but including a ‘simulation duration’ dimension as well. Certainly the evidence hints that more systems make the ‘switch’ from polynomial to exponential divergence as the duration of the simulation increases.

Our physical model is very simplistic, accounting only for Newtonian gravity between the Sun and Jovian planets. Although we ignore many physical effects which are known to affect the detailed motion of the planets (Laskar 1999; Varadi et al. 2003), it is unclear if such effects would substantially alter the chaotic nature of solutions. We at first believed that the largest such effect ignored was solar mass loss. Our first simulations did not account for solar mass loss, which amounts to about one part in 10^7 Myr^{-1} (Laskar 1999; Noerdlinger 2005). Since we find that perturbations in position of that order can shift the system in-and-out of chaos, a naive analysis might lead one to suspect that solar mass loss might shift

the planetary orbits in-and-out of resonance on a time-scales that is fast compared to the Lyapunov time, thus smoothing out the sibling divergence. We thus modified our model to include solar mass loss, but surprisingly it made absolutely no observable difference to any of the figures presented in this paper. To ensure that we did not make an error, we simulated systems with ever increasing mass loss until the Sun was losing 10 per cent of its mass per 100 Myr. We noted that the planetary orbital semimajor axes expanded significantly, as would be expected, but that the sibling divergences did not change until mass loss was at a rate of about 1 per cent per 100 Myr (1000 times greater than in reality). Thus, we conclude that solar mass loss also makes no difference to our results. Similarly, we believe that relativistic effects will have negligible effect on the existence or absence of chaos (Varadi et al. 2003).

5 CONCLUSION AND FUTURE WORK

There has been a discrepancy between various investigators as to the existence of chaos in the orbits of the Jovian planets. We have shown that the discrepancy can be explained because there genuinely exist both chaotic and regular orbits within observational error. In particular, we have shown that, within the volume of phase space enclosing the observational error of the current positions of the Jovian planets, there exist some ICs (about 70 per cent of them) that lead to chaotic orbits over a 200-Myr time-scale, and some (about 30 per cent of them) that show no evidence of chaos over 200 Myr.⁶ After 1 Gyr, about 10 per cent of ICs still show no evidence of chaos. Even after 5 Gyr, the ‘canonical’ IC from DE405 has a small enough Lyapunov exponent that it may be possible to predict the positions of the Jovian planets to within a few degrees in longitude, during the entire main-sequence lifetime of the Sun.

We have validated our results in several ways. First, we have performed convergence tests in all cases: compare Fig. 4 (unconverged) to Fig. 5 (converged); and the top curves of Fig. 8 (low precision but still converged) agree with the higher precision ones on the bottom. Secondly, we have confirmed the results of previous authors from both camps (Murray & Holman 1999; Grazier et al. 2005). Thirdly, we have utilized three very different double-precision integration methods, all of which agree with each other in the small time-step limit. Fourthly, we have verified that our integrations satisfy Brouwer’s law in the cases we expect them to. Fifthly, we have compared our double-precision solutions with quadruple precision integrations to verify the accuracy of the former.

We conclude that it is extremely unlikely that our results are substantially affected by numerical error.

ACKNOWLEDGMENTS

I thank Scott Tremaine, Norm Murray, Matt Holman, Philip Sharp and Bill Newman for helpful discussions and comments on the manuscript; Norm Murray and Philip Sharp for sending me (and explaining) their ICs and Ferenc Varadi for giving me the source code to his most recent version of NBI. The referee also provided many useful comments.

REFERENCES

- Barrio R., Blesa F., Lara M., 2005, *Comput. Math. Appl.*, 50, 93
Benettin G., Giorgilli A., 1994, *J. Stat. Phys.*, 74, 1117

⁶ It would be interesting to measure the percentage of astronomers who were on either side of the argument.

- Brouwer D., 1937, *AJ*, 46, 149
 Chambers J. E., 1999, *MNRAS*, 304, 793
 Channell P. J., Scovel C., 1990, *Nonlinearity*, 3, 231
 Goldstein D. J., 1996, PhD thesis, Department of Mathematics, UCLA
 Grazier K. R., 1997, PhD thesis, Department of Geophysics and Space Physics, UCLA
 Grazier K. R., Newman W. I., Kaula W. M., Varadi F., Hyman J. M., 1995, *BAAS*, 27, 829
 Grazier K. R., Newman W. I., Varadi F., Goldstein D. J., Kaula W. M., 1996, *BAAS*, 28, 1181
 Grazier K. R., Newman W. I., Kaula W. M., Hyman J. M., 1999, *Icarus*, 140, 341
 Grazier K. R., Newman W. I., Hyman J. M., Sharp P. W., 2005, *ANZIAM J.*, 46, C1086
 Guzzo M., 2001, *Celest. Mech. Dyn. Astron.*, 80, 63
 Guzzo M., 2005, *Icarus*, 174, 273
 Hayes W. B., 2007, *Nat. Phys.*, 3, 689
 Herbst B. M., Ablowitz M. J., 1989, *Phys. Rev. Lett.*, 62, 2065
 Ito T., Tanikawa K., 2002, *MNRAS*, 336, 483
 Jorba A., Zou M., 2005, *Exp. Math.*, 14, 99
 Kinoshita H., Nakai H., 1996, *Earth Moon Planets*, 72, 165
 Laskar J., 1989, *Nat*, 338, 237
 Laskar J., 1990, *Icarus*, 88, 266
 Laskar J., 1994, *A&A*, 287, L9
 Laskar J., 1996, *Celest. Mech. Dyn. Astron.*, 64, 115
 Laskar J., 1997, *A&A*, 317, L75
 Laskar J., 1999, *R. Soc. Lond. Phil. Trans. Ser. A*, 357, 1735
 Lecar M., Franklin F. A., Holman M. J., Murray N. W., 2001, *ARA&A*, 39, 581
 Lessnick M. K., 1996, PhD thesis, UCLA
 Lichtenberg A. J., Lieberman M. A., 1992, *Regular and Chaotic Dynamics*. Springer-Verlag, Berlin
 Lissauer J. J., 1999, *Rev. Mod. Phys.*, 71, 835
 Mandelbrot B., 1982, *The Fractal Geometry of Nature*. Freeman & Co., San Francisco
 Morrison L. V., Evans D. W., 1998, *A&AS*, 132, 381
 Murison M. A., 1989, *AJ*, 98, 2346
 Murray N., Holman M., 1999, *Sci*, 283, 1877
 Murray N., Holman M., 2001, *Nat*, 410, 773
 Newman W. I., Lee A. Y., 2005, *BAAS*, 37, 531
 Newman W. I., Varadi F., Lee A. Y., Kaula W. M., Grazier K. R., Hyman J. M., 2000, *BAAS*, 32, 859
 Noerdlinger P. D., 2005, *Solar Mass Loss, the Astronomical Unit, and the Scale of the Solar System*: <http://home.comcast.net/pdnoerd/SMassLoss.html>
 Rauch K. P., Holman M., 1999, *AJ*, 117, 1087
 Reich S., 1999, *SIAM J. Numer. Anal.*, 36, 1549
 Saha P., Tremaine S., 1992, *AJ*, 104, 1633
 Sanz-Serna J. M., 1992, in Iserles A., ed., *Acta Numerica*. Cambridge Univ. Press, Cambridge, p. 243
 Standish E. M., 1998, *JPL Planetary and Lunar Ephemerides, DE405/LE405*. JPL IOM 312.F-98-048. Available at <http://ssd.jpl.nasa.gov/iau-comm4/relateds.html>
 Sussman G. J., Wisdom J., 1988, *Sci*, 241, 433
 Sussman G. J., Wisdom J., 1992, *Sci*, 257, 56
 Varadi F., Runnegar B., Ghil M., 2003, *ApJ*, 592, 620
 Wisdom J., 2006, *AJ*, 131, 2294
 Wisdom J., Holman M., 1991, *AJ*, 102, 1528
 Wisdom J., Holman M., Touma J., 1996, *Fields Inst. Commun.*, 10, 217

This paper has been typeset from a $\text{\TeX}/\text{\LaTeX}$ file prepared by the author.